instance, several studies have hinted at a significant contribution of oxidized uracil derivatives, such as 5-hydroxyuracil (5-OH-U) or uracil glycol (Ug), to G:C to A:T transitions in *E. coli*. An initial oxidation of cytosine is followed by deamination to a poorly repaired uracil derivative, which is one of the most frequent forms of endogenous DNA damage and strongly miscoded during replication (17). The hydrolytic deamination of 5-methyl cytosine (5mC) to thymine generates a thymine mispaired with guanine (18). Mutations resulting from 5mC comprise one of the most frequent classes of point mutation found in human cancer cells (19). The damaged pyrimidines are generally removed by glycosylases that cleave the bond between the sugar and N1 position of the damaged base (20). In the human genome, several different glycosylases with uracil-DNA glycosylase activity have been identified, and many of these share substantial homology with uracil DNA glycosylases found in other organisms (20).

In *E. coli*, Nth glycosylase, or endonuclease III (Endo III), and Nei glycosylase, or endonuclease VIII (Endo VIII), are base excision repair proteins with overlapping substrate specificities that remove oxidized pyrimidine bases from DNA (21,22). Upon the recognition of an oxidized pyrimidine by a DNA glycosylase, the *N*-glycosylic bond is cleaved, releasing the free base. This event is followed by the cleavage of the phosphodiester backbone by an associated DNA lyase activity, which leaves a blocked 3′ terminus in the resulting nick (23). The block, either an α,β-unsaturated aldehyde or a phosphate, must be removed by the phosphodiesterase or phosphatase activity of another class of enzymes, the 5′ AP endonucleases. This phenomenon results in a single base gap, which is filled in by DNA polymerase and sealed by DNA ligase (24). Endo III and Endo VIII remove potentially lethal lesions, such as thymine glycol and urea, that are blocks to DNA synthesis *in vitro* and lethal *in vivo* (25,26). Endo III and VIII also remove free radical damaged cytosines, Ug, dihydrouracil, 5-OH-U, and 5-hydroxycytosine, all of which are mutagenic (17,27) and can mispair with adenosine during DNA synthesis *in vitro* (28).

We previously reported that *Salmonella typhimurium* strains YG3001, YG3002, and YG3003 are highly sensitive to oxidative mutagens due to a lack of $mutM_{ST}$ encoding FPG (29). The strains are derivatives of Ames tester strains TA1535, TA1975, and TA102, respectively, which are widely used for the identification of environmental mutagens and carcinogens. In this study, we disrupted the genes encoding Endo III and Endo VIII in *S. typhimurium* TA1535, i.e., nth_{ST} and nei_{ST}, respectively, to establish strain YG3206. To evaluate chemical sensitivity, we selected well-known oxidative agents and those reported to be mutagenic in the tester strains sensitive to oxidative mutagens (30,31). The references therein also suggested some chemicals to be screened. Because strains YG3206 and YG3001 lack Nth/Nei and FPG, respectively, we expected that a comparison of sensitivities would identify chemicals that preferably oxidize pyrimidines or purines in DNA. Our results suggest that L-cysteine and four other chemicals may predominantly oxidize pyrimidines in DNA, thereby inducing mutations. In contrast, potassium bromate and three other chemicals seem mainly to oxidize purines in DNA. Collectively, the results suggest that the chemicals induce oxidative mutagenesis through different mechanisms, and that newly established strains YG3206 and YG3216 are useful for identifying chemicals that induce mutations through the oxidation of pyrimidine in DNA.

Materials and Methods

Strains and plasmids: The strains and plasmids used in this study are listed in Table 1.

Oligonucleotides: Oligonucleotides used for PCR amplification were purchased from Japan Bioservice (Ibaraki, Japan). Each sequence is shown in the text. The one including a thymine glycol used for DNA glycosylase assay was commercially obtained from Tsukuba Oligo Service Co., Ltd. (Tsukuba, Japan), where the oligonucleotide was applied on a poly acrylamide gel, then the corresponding band was purified from the gel after running.

Media: Luria-Bertani broth and agar were used for bacterial culture. Vogel-Bonner minimal agar plates and top agar were prepared as previously described (32) and used for the His^+ reversion assay with *S. typhimurium*. Nutrient broth (Difco, MI, U.S.A.) was used in the precultures for the reversion assay. Ampicillin (Ap, 50 μg/mL), kanamycin (Km, 25 μg/mL), or chloramphenicol (Cm, 10 μg/mL) were supplemented in overnight cultures for strains harboring pKM101, $\Delta mutM$::*kan*, or Δnei_{ST}::*cat*, respectively. Liver S9 prepared from male Sprague-Dawley rats pretreated with phenobarbital and 5,6-benzoflavone was purchased from Kikkoman Cooperation (Chiba, Japan).

Construction of the Endo III-deficient strain: We introduced a stop codon, TGA, in the coding region of nth_{ST} in TA1535 without any drug-resistance marker (33). The nth_{ST} gene and its flanking region were amplified by PCR using the chromosome DNA of TA1535 and the primers 5′-CAC AAC GCT GGT ATT AAC GCT GAC-3′ and 5′-GCA CTG AAG GAA GAG AAA AGG GTG-3′, and then cloned into an *Aat*II site of the pBR322 vector. The resultant plasmid, pYG433, was digested with *Sca*I and *Eco*RV, and the resulting 2-kb fragment was sub-cloned into *Sma*I site of the pKO3 vector (Table 1). The pKO3 vector has *cat* and *sacB*, used for selection as described below. The resultant plasmid, pYG437, included nth_{ST} and was

Table 1. List of the strains and plasmids used in this study

	Genetic characteristics	Source
Strain		
TA1535	*hisG46, gal,* Δ(*chl, uvrB bio*) *rfa*	(32)
YG3001	The same as TA1535, but deficient in $mutM_{ST}$, Km^R	(29)
YG3201	The same as TA1535, but deficient in nei_{ST}, Cm^R	This study
YG3203	The same as TA1535, but deficient in nth_{ST}	This study
YG3206	The same as TA1535, but deficient in nth_{ST} and nei_{ST}, Cm^R	This study
TA100	The same as TA1535, but harbors pKM101, Ap^R	(32)
YG3008	The same as TA3001, but harbors pKM101, Ap^R, Km^R	(29)
YG3216	The same as TA3206, but harbors pKM101, Ap^R, Cm^R	This study
Plasmid		
pYG432	derivative of pBR322, carrying nei_{ST} at the *Aat*II site, Tc^R	This study
pYG434	derivative of pBR322, carrying nei_{ST} disrupted with *cat*-replacement, Cm^R, Tc^R	This study
pYG433	derivative of pBR322, carrying nth_{ST} at the *Aat*II site, Tc^R	This study
pYG437	derivative of pKO3, subcloning the *Sca*I-*Eco*RV fragment, including nth_{ST} from pYG433, into the *Sma*I site, Cm^R	This study
pYG438	derivative of pKO3, carrying nth_{ST} which has a four-base deletion, Cm^R	This study
pBR322	vector plasmid, Ap^R, Tc^R	Laboratory stock
pKO3	vector plasmid with temperature-sensitive replication origin, Cm^R	(33)

Km^R, kanamycin resistant; Cm^R, chloramphenicol resistant; Ap^R, ampicillin resistant; Tc^R, tetracycline resistant.

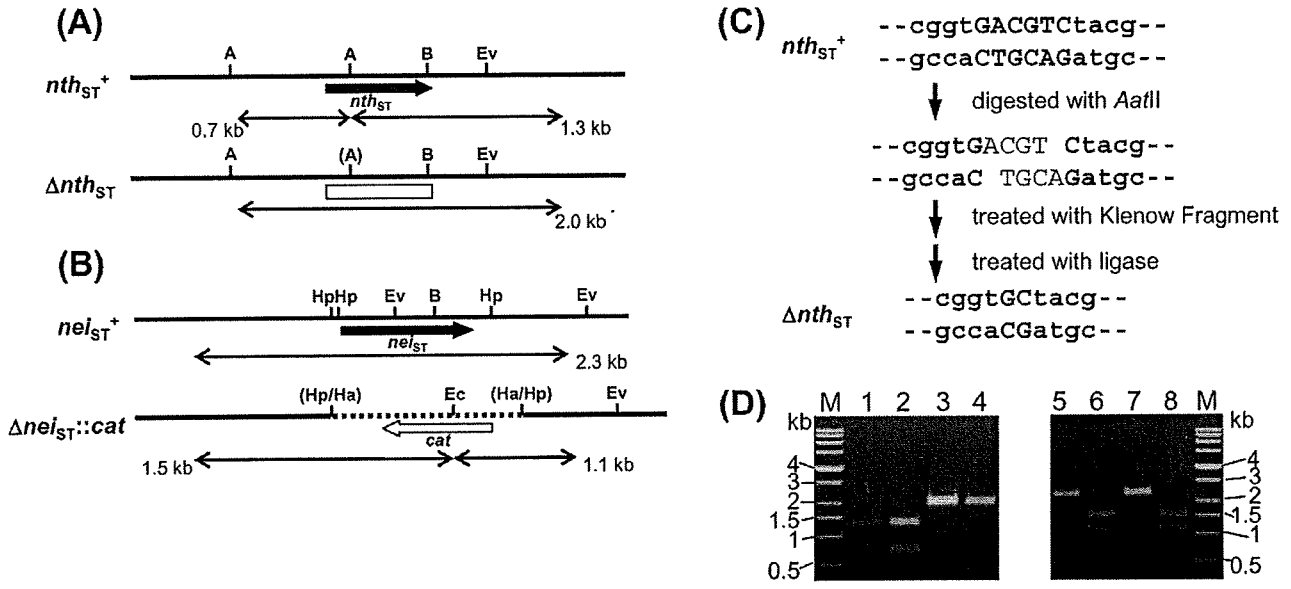

Fig. 1. Disruption of the nth_{ST} and nei_{ST} genes. Partial restriction maps of nth_{ST} (A) and nei_{ST} (B) and the surrounding chromosomal region in the original TA1535 strain and its deletion recombinants. Thick black arrows indicate the position and transcriptional direction of the genes in wild-type (A) and (B). The white box (A) exhibits a deficient nth_{ST} gene possessing the introduced frameshift mutation. The dotted line (B) indicates the replaced fragment, including the *cat* gene shown with a white arrow. The size of the bands amplified by PCR or digested with restriction enzymes after the PCR reaction is shown at each line in (A) and (B). Restriction enzyme sites are shown as follows: A, *Aat*II; (A), missing *Aat*II site; B, *Bgl*II; Ec, *Eco*RI; Ev, *Eco*RV; Ha, *Hae*II; Hp, *Hpa*I. (Hp/Ha) and (Ha/Hp) represent the junctions of the *Hae*II fragment when it was inserted into the *Hpa*I site in nei_{ST}. (C) The scheme shows how to produce the deletion/frameshift in nth_{ST} at the *Aat*II site, i.e., GACGTC. Four base pairs, ACGT, are deleted at the end of the procedure. (D) The pictures of the agarose gel exhibit the bands after restriction enzyme digestions. Left: *Aat*II digestion for Δnth_{ST} strain construction. Right: *Eco*RI digestion for Δnei_{ST} strain construction. M, size marker; lanes 1 and 5, TA1535; lanes 2 and 6, YG3201; lanes 3 and 7, YG3203; lanes 4 and 8, YG3206.

digested with *Aat*II (Takara Bio, Ootsu, Japan) (Fig. 1A). The cleaved plasmid was treated with Klenow fragment (New England Biolabs) to make both ends blunt (Fig. 1C). After ligation of the ends, four bases (ACGT) were deleted, which generated a TGA at the 46th codon of nth_{ST}. The obtained plasmid, pYG438, was introduced into TA1535, and Cm-resistant colonies were selected at 43°C to identify clones in which the plasmid was integrated into the chromosome. Then, the Cm-resistant colonies were examined to determine whether

they could survive on LB plates with 5% sucrose. Only clones in which the integrated *sacB*-containing fragment was removed were able to form colonies on the plates because the *sacB* gene product converts sucrose to a toxic substance. The lack of ACGT in nth_{ST} was verified by digestion of the PCR product with the *Aat*II restriction enzyme, followed by 0.8% agarose gel electrophoresis (Fig. 1D). The clones with PCR products tolerant to *Aat*II digestion were designated as YG3203, i.e., TA1535 Δnth_{ST}. The set of primers used for amplification were the same as for cloning.

Construction of the Endo VIII-deficient strain: The nei_{ST} gene and its flanking region, with a total size of 2.3 kb, was amplified by PCR using the chromosome DNA of TA1535 and primers 5′-GTA TTT GCT GGT TCT TTA GGT GCG C-3′ and 5′-GTG ATC TGG TTT CCG CCG CTT A-3′, and the amplified fragment was cloned into an *Aat*II site of the pBR322 vector. Using the resultant plasmid, pYG432 (Table 1), nei_{ST} was disrupted by the pre-ligation method (34). Briefly, pYG432 was digested with the *Hpa*I enzyme, and an approximate 1-kb region containing nei_{ST} was replaced with a *cat* gene cassette (Fig. 1B). The resultant plasmid, pYG434, was digested with *Apa*LI, and T4 DNA ligase joined both ends of the 5-kb fragment. The treated DNA was introduced into TA1535 and Cm-resistant

Table 2. List of the chemicals used in this study

	Chemical	CAS registry number	Molecular weight	Solvent	Source†
1	L-cysteine	52-90-4	121.15	H_2O	Wako
2	L-penicillamine	1113-41-3	149.21	H_2O	TCI
3	Dopamine-HCl	62-31-7	189.64	H_2O	Wako
4	Phenazine methosulfate (PMS)	3130-59-4	306.34	H_2O	Wako
5	Hydrogen peroxide (H_2O_2)	7722-84-1	34.01	H_2O	Wako
6	Phenazine ethosulfate (PES)	10510-77-7	334.39	H_2O	Dr. Ohta
7	Potassium bromate ($KBrO_3$)	7758-01-2	167.00	H_2O	Wako
8	Methylene blue (MB)*	61-73-4	319.86	H_2O	Sigma
9	Neutral red (NR)*	553-24-2	288.78	H_2O	Sigma
10	Benzo[*a*]pyrene (B[*a*]P)*	50-32-8	252.31	DMSO	Wako
11	2-Nitrofluorene	607-57-8	211.22	DMSO	TCI
12	Glyoxal	83513-30-8	58.04	H_2O	TCI
13	Kethoxal	27762-78-3	148.16	DMSO	Sigma
14	Methylglyoxal	78-98-8	72.06	H_2O	Sigma
15	*N*-Nitrosotaurocholic acid (*N*-NTCA)	82660-96-6	544.70	H_2O	Dr. Totsuka
16	Paraquat	2074-50-2	257.16	H_2O	Wako
17	Phenylhydrazine	100-63-0	108.14	DMSO	Wako
18	Hydroquinone	123-31-9	110.11	H_2O	Wako
19	2,6-Dimethyl-1,4-benzoquinone	527-61-7	136.15	DMSO(10 mg/mL)→W+	Wako
20	Duroquinone	527-17-3	166.22	DMSO(1 mg/mL)→W	Wako
21	Menadione	58-27-5	172.18	DMSO(1 mg/mL)→W	Wako
22	Lawsone (2-hydroxy-1,4-naphthoquinone)	83-72-7	174.15	DMSO(5 mg/mL)→W	TCI
23	Acetaldehyde	75-07-0	44.05	H_2O	Merck
24	Methoxsalen	298-81-7	216.19	DMSO	Sigma
25	Catechol	120-80-9	110.11	H_2O	TCI
26	2,5-Toluquinone	553-97-9	122.12	DMSO(20 mg/mL)→W	Wako
27	1,4-Benzoquinone	106-51-4	108.09	DMSO(10 mg/mL)→W	Wako
28	l-Dopa	59-92-7	197.19	0.5N NaOH(50 mg/mL)→W	TCI
29	Cumene hydroperoxide	80-15-9	152.2	DMSO(5 mg/mL)→W	Aldrich
30	*t*-Butyl hydroperoxide	75-91-2	90.12	H_2O	Wako
31	4-Oxo-2-hexenal	2492-43-5	112	DMSO	Dr. Kawai
32	Psolaren	66-97-7	186.16	DMSO	Sigma
33	Spermine NONOate	136587-13-8	262.4	0.1N NaOH(5 mg/mL)→W	Sigma
34	*S*-nitroso-*N*-acetyl-dl-penicillamine	79032-48-7	220.25	DMSO	Sigma
35	1,3-Butadiene diepoxide	1464-53-5	86.09	DMSO	Wako
36	Formaldehyde	50-00-0	30.03	H_2O	Wako
37	Glutaraldehyde	111-30-8	100.12	H_2O	Wako
38	Plumbagin	481-42-5	188.18	DMSO	TCI
39	Bleomycin hydrochloride	67763-87-5	1453.02	H_2O	Wako
40	Thiabendazole	148-79-8	201.3	DMSO	Wako

*: These chemicals were used for visible light irradiation assay.
†: Wako, Wako Pure Chemicals; Sigma or Aldrich, Sigma-Aldrich Chemicals; TCI, Tokyo Chemical Industry.
+: "→W" means that the chemical was initially dissolved in DMSO or NaOH solution, then diluted with water according to its solubility.

colonies were selected. The *Eco*RI site is present only in *cat* and not in nei_{ST} (Fig. 1B). The replacement of nei_{ST} with *cat* was confirmed by PCR amplification using the cloning primers, followed by digestion with *Eco*RI (Fig. 1D). The resultant strain, TA1535 with Δnei_{ST}::*cat*, was designated as YG3201. In the same way, YG3206, i.e., TA1535$\Delta nth_{ST}\Delta nei_{ST}$::*cat*, was constructed using YG3203 instead of TA1535 (Fig. 1D). Introducing pKM101 into YG3206 resulted in YG3216, i.e., TA1535$\Delta nth_{ST}\Delta nei_{ST}$::*cat*/pKM101 (Table 1).

DNA cleavage assay: Crude lysate was prepared from a 40-mL culture at an OD_{600} of 0.6–0.7 as previously described (35). One picomole of each Cy3-labeled duplex oligonucleotide (5′-Cy3-CTC GTC AGC ATC T TgC ATC ATA CAG TCA GTG-3′ and 3′-GAG CAG TCG TAG AAG TAG TAT GTC AGT CAC-5′, Tg is thymine glycol) were incubated at 37°C for 30 min with various amounts of the crude lysate derived from TA1535, YG3201, YG3203, or YG3206 in 10 μL reaction mixtures containing 10 mM Tris-HCl (pH 7.5), 1 mM EDTA, 100 mM NaCl, and 0.1 mg/mL BSA. The crude lysate was diluted to include 1, 3, or 10 μg of protein in each reaction. Strain AB1157 of *E. coli* was used in the same way as a positive control of crude lysate because it has both glycosylase activities. After incubation, the reactions were terminated by the addition of loading buffer (98% formamide, 10 mM EDTA, 20 mg/mL blue dextran). The samples were then heated at 95°C for 5 min and immediately cooled on ice. The samples were loaded onto 15% polyacrylamide denaturing gels containing 8 M urea. After electrophoresis at 2000 V, the gels were scanned by the Molecular Imager FX Pro System (BioRad, USA) to detect Cy3 fluorescence. The intensity of each band was determined by Quantity One software (BioRad). As a control, purified Endo III (1 unit) and Endo VIII (10 units) (New England Biolabs, USA) were used.

Chemicals: The names, abbreviations, CAS registry numbers, molecular weight, solvent to dissolve the chemicals, and sources of the chemicals assayed in this study are listed in Table 2. Phenazine ethosulfate, *N*-nitrosotaurocholic acid, and 4-oxo-2-hexenal were kindly provided by Drs. Toshihiro Ohta from Tokyo University of Pharmacy and Life Sciences, Yukari Totsuka in National Cancer Center Research Institute, Tokyo, and Kazuaki Kawai in University of Occupational and Environmental Health Japan, Kitakyushu, respectively.

Mutagenicity assay: The mutagenicity assay was carried out with a pre-incubation procedure (32). Briefly, 0.1 mL of overnight culture was incubated with the chemicals dissolved in 0.1 mL of solvent and 0.5 mL of 1/15 M phosphate buffer (pH 7.4) for 20 min at 37°C. The S9 mix was added instead of the buffer for the assay using methylene blue (MB). The mixture was then poured onto agar plates with soft agar and incubated for 2 days at 37°C in the dark. Each chemical was assayed with 4–7 doses on triplicate plates with six strains, TA1535, YG3001, YG3206, TA100, YG3008, YG3216, in parallel.

White fluorescent light irradiation: Methylene blue, neutral red (NR), and benzo[*a*]pyrene (B[*a*]P) were subjected to the assay with plates that were irradiated with white fluorescent light, which was delivered by a fluorescent lamp (15W, 370–750 nm wavelength) during the 2-day incubation at 37°C. The plates were placed upside down 50 cm from the light source. The light intensity of 1,000 lx was measured with an Illumination meter (IM-1, Tokyo Kogaku Kikai K.K., Tokyo, Japan). Plates not exposed to light were covered with sheets of aluminum foil during the incubation. In addition, room lights were turned off during the experiments to distinguish between the results with- and without-irradiation conditions. Spontaneous mutagenicity in the irradiated-condition was also examined in this manner.

Results

Establishment of *S. typhimurium* strains deficient in Endo III and/or VIII: Our aim was to develop a system to identify chemicals that cause mutations via oxidized pyrimidines. The gene encoding Endo III (nth_{ST}^{+}) was disrupted by recombination and confirmed by PCR and restriction-enzyme digestion. *Aat*II digestion cleaved the 2-kb DNA fragment containing the nth_{ST} from the parental strain, TA1535, into two fragments 1.3 kb and 0.7 kb in size (Figs. 1A and D, Lane 1), whereas the fragment amplified with the same primers from the nth_{ST}-disrupted strain was not cleaved, which is consistent with the expected loss of the *Aat*II site in the disruptant (Figs. 1A, C and D, Lane 3). The nth_{ST}-disrupted strain was designated YG3203. A similar approach was used to inactivate nei_{ST} in TA1535 (Fig. 1B) to generate YG3201. *Eco*RI digestion did not cleave the fragment from the parental strain (Fig. 1D, Lane 5), whereas the same fragment from the nei_{ST}-disrupted strain was cleaved into two fragments 1.5 kb and 1.1 kb in size (Fig. 1D, Lane 6). This finding is consistent with the expected addition of the *Eco*RI site derived from the insertion of *cat* in the disruptant (Fig. 1B). The nth_{ST}/nei_{ST} double mutant, designated YG3206, was obtained by introducing nei_{ST}::*cat* into YG3203 (Fig. 1D, Lanes 4 and 8).

We examined whether the strains appropriately lost the endonuclease activities for the substrates (Fig. 2). The endonuclease activities were detected in the crude extracts of parental strain TA1535 and *E. coli* strain AB1157, which possesses counterparts to Endo III and VIII. The positions of nicked products I and II (35) formed by treatment with the crude extracts of TA1535 and AB1157 (Fig. 2, Lanes 4–6 and 16–18) were identi-

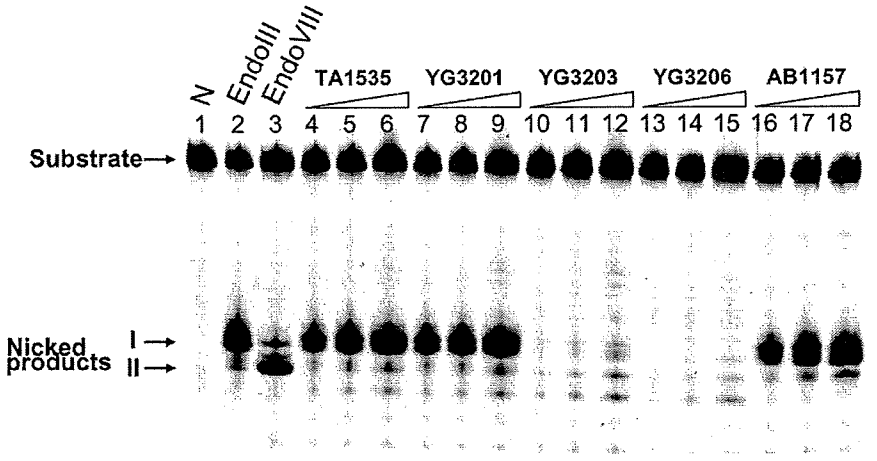

Fig. 2. PAGE analysis of the reaction products formed by the incubation of oligonucleotide substrates containing thymine glycol with Endo III and Endo VIII or crude lysates. The annealed oligonucleotides were incubated with different amounts of the indicated enzymes or crude lysates at 37°C for 30 min. Nicked products were separated by 15% denaturing PAGE. The image of the gel is shown. Lane 1, primer without reaction; lane 2, Endo III; lane 3, Endo VIII; lanes 4-6, TA1535; lanes 7-9, YG3201; lanes 10-12, YG3203; lanes 13-15, YG3206; lanes 16-18, AB1157. Three arrows indicate, in order starting from the top, the position of substrate, product I for Endo III activity, and product II for Endo VIII activity.

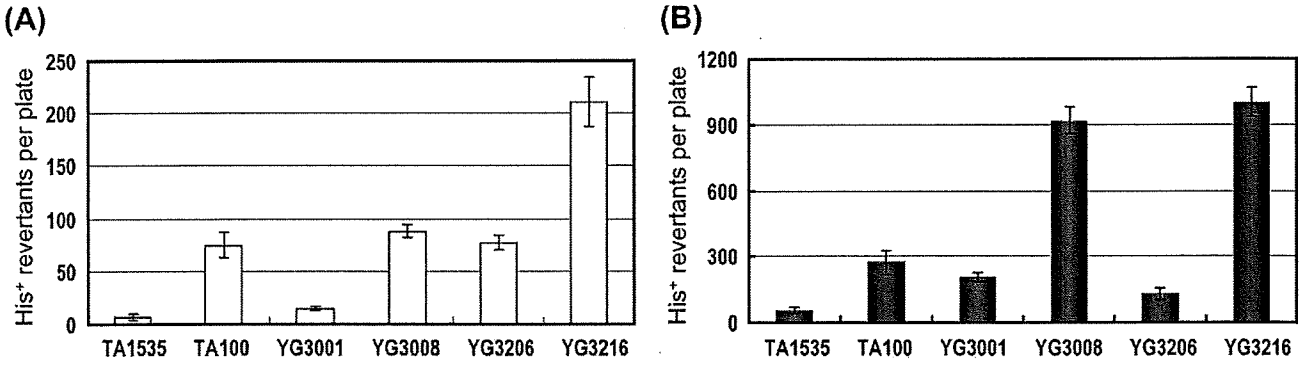

Fig. 3. Spontaneous mutagenicity in *S. typhimurium* strains deficient in DNA glycosylases. The assay was carried out in the dark (A) and under irradiation with a fluorescent light (B) as described in Materials and Methods. Strains are indicated at the bottom of the graphs. The height of bars represents the numbers of spontaneous His^+ revertants per plate and the standard deviations.

cal to the bands generated by the treatment of the substrate with purchased Endo III and VIII (Fig. 2, Lanes 2 and 3). Comparing nicked product I in the lanes for TA1535 and AB1157 with those of YG3203 and YG3206, it is clear that strains YG3203 and YG3206 lost Endo III activity (Fig. 2, Lanes 10-15). Comparing the bands at the position of nicked product II, YG3206 also lost Endo VIII activity (Fig. 2, Lanes 13-15). Thus, we conclude that YG3206 lost both Endo III and VIII activities.

Spontaneous mutagenesis: The number of spontaneous His^+ revertants per plate was examined in the newly constructed strain YG3206, $\Delta nth_{ST}\Delta nei_{ST}$, and five reference strains: the TA1535 parent strain, its $\Delta mutM_{ST}$ derivative, YG3001, and their respective pKM101-harboring strains, TA100 and YG3008. We also included YG3216, the pKM101-harboring version of YG3206. The plasmid pKM101 works for efficient bypasses of DNA lesions caused by chemicals. These results are summarized in Fig. 3. For YG3206, $\Delta nth_{ST}\Delta nei_{ST}$, there were 82 ± 16 revertants per plate; for YG3001 and TA1535, the values were 19 ± 4 and 6 ± 2, respectively (Fig. 3A). To further validate these strains, we determined the effect of fluorescent light on their spontaneous mutation frequencies. In the absence of any other exogenous DNA-damaging treatment, irradiation alone enhanced mutation by more than 10-fold in YG3001, roughly two-fold in YG3206, and 10-fold in TA1535 (Fig. 3B). Irrespective of irradiation, the pKM101-harboring strains produced more revertants than their respective non-pKM101 strains.

Specificity and sensitivity of YG3206: The mutagenicity of 40 chemicals (Table 2) was compared among the six strains mentioned above (Table 1). Two-thirds of the tested chemicals were not mutagenic in any of the strains and exhibited neither dose responses nor 2-fold

Table 3. Mutagenic sensitivity to the chemicals in *S. typhimurium* strains deficient in $mutM_{ST}$ or nei_{ST}/nth_{ST}

Chemicals	Group*	TA1535	YG3001	YG3206	Dose† (μg/plate)	TA100	YG3008	YG3216	Dose† (μg/plate)
		Induced His^+ revertants per μmol chemical				Induced His^+ revertants per μmol chemical			
L-cysteine	A	ND‡	ND	6.5	2500	11	17	130	500
L-penicillamine	A	ND	1.1	57	2000	8.3	12	170	1000
Dopamine-HCl	A	ND	ND	21§	500	ND	ND	230	100
PMS	A	ND	ND	3,400§	5	ND	ND	9,800§	5
H_2O_2	A	ND	ND	238,000	0.02	116,000§	252,000§	1,153,000§	0.01
PES	A′	ND	ND	ND		ND	ND	3,700	25
$KBrO_3$	B	ND	1.2	ND	2500	ND	ND	ND	
MB + S9 + light	B	400	5,700	ND	25	7,200	14,000	ND	25
NR + light	B	8,200	51,000	19,000	1	22,000	51,000§	64,000§	1
B[*a*]P + light	B	1,600	8,900	1,300	10	14,000	39,000	11,000	10
2-Nitrofluorene	C	ND	ND	ND		36,000	23,000	66,000	5
Glyoxal	C	ND	ND	ND		510	510	1,000	50
Kethoxal	C	ND	ND	ND		24,000	2,900	7,400	10
Methylglyoxal	C	ND	ND	ND		13,000	800	2,500	10
N-NTCA	D	11,000	11,000	10,000	50	—‖	—	10,000	50

These results were confirmed at least three times. The numbers are the mean values of induced His^+ revertants per μmol chemical in triplicate plates or three independent assays with a single plate.

*: The definition is in the text.

†: Dose used for calculation of the numbers of induced His^+ revertants in the category.

‡: ND: No mutagenicity was detected, which means no dose response and less than 2-fold increase in the number of induced His^+ revertants per plate.

§: These values were not 2-fold more than those for the solvent control, but the results indicated a clear dose-response in the number of induced His^+ revertants per plate.

‖: The dash indicates that the value was not examined.

increases in the number of His^+ revertants per plate (data not shown). The chemicals listed in Table 3 were mutagenic in some or all of the strains tested. Based on the order of strain sensitivity, we classified the chemicals into Groups A to D as follows.

Group A compounds: L-cysteine, L-penicillamine, dopamine-HCl, phenazine methosulfate (PMS), and H_2O_2 exhibited significant mutagenicity in Endo III/VIII-deficient strains, i.e., YG3206 and YG3216, but not in the Endo III/VIII-proficient and FPG-deficient strains, i.e., YG3001 and YG3008 (Fig. 4). Phenazine ethosulfate (PES) exhibited mutagenicity only in YG3216 but not in YG3206 or the other strains. Thus, we categorized it into Group A′ (Table 3).

Group B compounds: Potassium bromate, MB plus visible light with the S9 mix, NR plus visible light, and B[*a*]P plus visible light (Table 3, Fig. 4) were more mutagenic in YG3001 than TA1535 and YG3206. The presence of pKM101 enhanced the mutagenicity of all Group B compounds except potassium bromate (Table 3, Fig. 4B).

Group C compounds: The mutagenicity of Group C compounds was dependent on the presence of pKM101 (Table 3). In these cases, the mutagenicity appeared unrelated to glycosylase deficiency; some were more mutagenic in YG3216 and others were more mutagenic in TA100.

In addition, *N*-nitrosotaurocholic acid (*N*-NTCA) was significantly mutagenic independent of DNA glycosylase status and without pKM101. This chemical was placed in a separate group, Group D (Table 3).

Discussion

Genetically engineered Ames tester strains are useful tools in environmental genotoxicology because they provide both extreme sensitivity and mechanistic information (36,37). For example, *S. typhimurium* strains YG7104 and YG7108, in which the repair systems for DNA damage by alkylating agents are disrupted, are hypersensitive to alkylating agents such as methyl

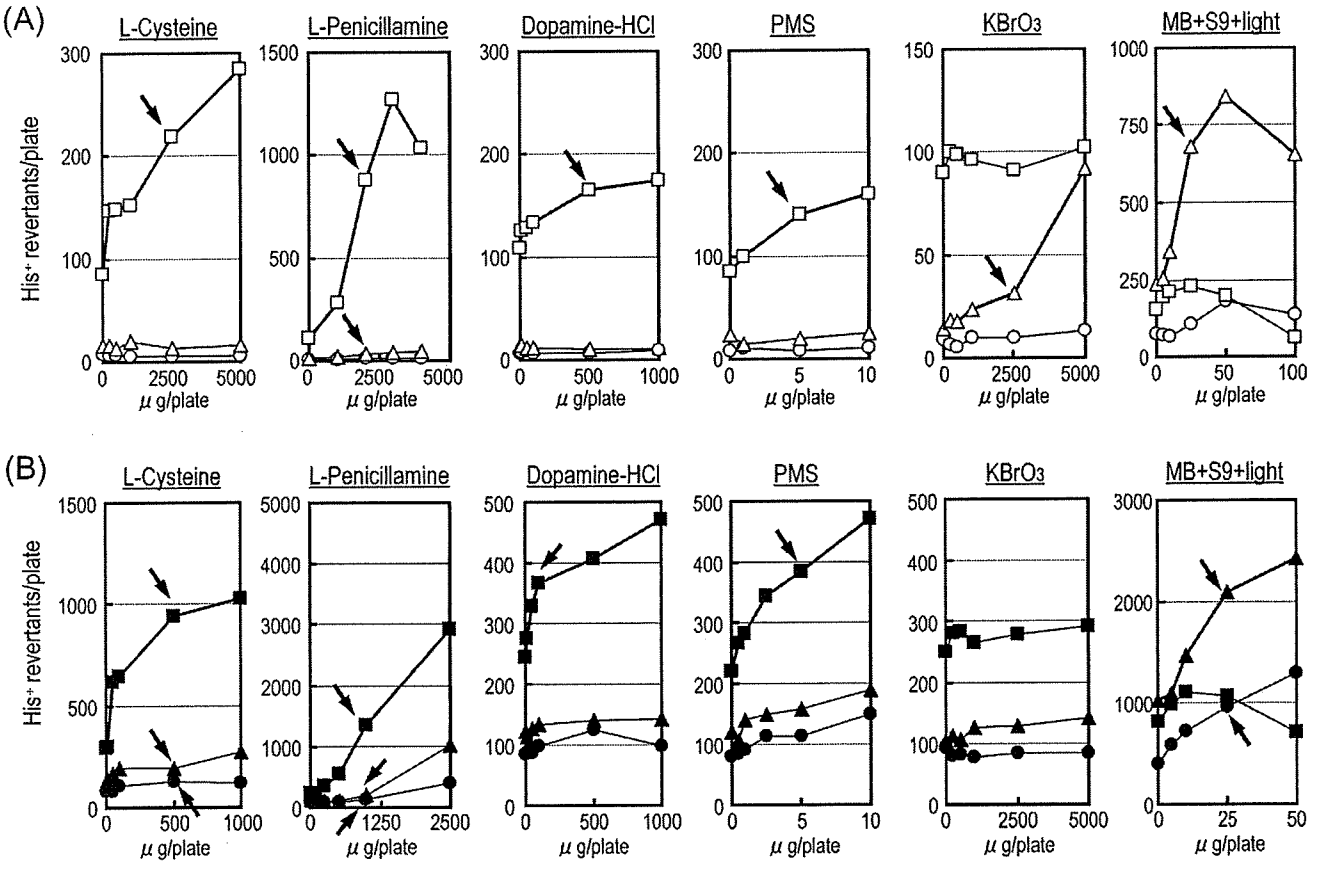

Fig. 4. Mutagenic responses of new *S. typhimurium* strains in the Ames test. The typical results for the test chemicals categorized into Groups A and B are indicated in (A) for the strains without pKM101 and (B) for the strains with pKM101 (Table 3). The number of His^+ revertants per plate was plotted against chemical dose in μg per plate. Symbols in (A): TA1535, ○; YG3001, △; YG3206, □. Symbols in (B): TA100, ●; YG3008, ▲; YG3216, ■. The arrows show the plot used for the calculation of the numbers shown in Table 3.

methanesulfonate and dimethylnitrosamine (38), and are used to investigate the mechanisms of chemical mutagenesis by this class of compounds (39,40). To expand the range of this research approach, we also established *S. typhimurium* strain YG5185, which can detect genotoxic PAHs with high specificity and sensitivity (41).

In the present study, we constructed strains YG3206 and YG3216, both of which lack two DNA glycosylases active on oxidized DNA pyrimidines. During the characterization of these strains, we noted that YG3206 exhibited specific sensitivity to the mutagenicity of L-cysteine; L-penicillamine; that is, dimethy L-cysteine; and dopamine-HCl. It is interesting that such naturally occurring compounds in organisms showed positive responses in the Ames tester strain. Similar findings have already been reported (42–44). Glatt reported the mutagenicity of L-cysteine and glutathione (GSH) in TA97, TA92, and TA104 with metabolic activation (42). Because the strains are not particularly sensitive to ROS, and catalase and superoxide dismutase did not inhibit the mutagenicity of GSH in TA92, Glatt concluded that ROS are not the cause of the L-cysteine and GSH mutagenicity. Our finding that YG3001 is not sensitive to the L-cysteine mutagenicity also suggests that high levels of 8-OH-G were not induced by cysteine. On the other hand, it has been reported that the mutagenicity of GSH and L-cysteine is oxidative in nature and involves ROS and/or other free radicals (43). Stark *et al.* proposed a mechanism for thiol mutagenesis: cysteine is converted to thiyl compounds, which react with transition metals and molecular oxygen and lead to produce H_2O_2 (43). Interestingly, H_2O_2 exhibited a similar pattern of mutagenicity with the tester strains as cysteine under our experimental conditions (Table 3). Both chemicals displayed mutagenicity in strain YG3206 but not TA1535 and YG3001, and the mutagenicity was enhanced by the introduction of pKM101. Therefore, it may be possible that cysteine generates H_2O_2, thereby oxidizing pyrimidines in DNA, which leads to mutations. Because we examined the mutagenicity of cysteine in the absence of S9 mix, the mechanism of mutation induction by cysteine may be different from those proposed by Glatt, who used S9 mix for the mutagenici-

ty assays of cysteine and GSH. Obviously, further work is needed to fully understand the mechanisms underlying the mutagenicity of cysteine and other chemicals in Group A.

As previously reported (29), H_2O_2 was not mutagenic in YG3001, a *mutM*$_{ST}$-deficient derivative of strain TA1535, but it was mutagenic in YG3003, a *mutM*$_{ST}$-deficient derivative of strain TA102. The reason that H_2O_2 was mutagenic in strain YG3003 is, perhaps, that the strain has an A:T base pair as its reversion target on multi-copy-number plasmid pAQ1. H_2O_2 exhibited mutagenicity in YG3206, which lacks both Endo III and Endo VIII activities (Table 3). Therefore, we suggest that H_2O_2 mainly induces oxidized pyrimidines in DNA. It may be interesting to construct a strain deficient in *nth*$_{ST}$ and *nei*$_{ST}$ and has an A:T base pair as a target for sensitive detection of H_2O_2 mutagenicity. Another noted result for H_2O_2 is that the introduction of pKM101 enhanced mutagenicity, even in the backgrounds of TA1535 and YG3001 (Table 3). The plasmid pKM101 encodes DNA polymerase, pol R1, which bypasses a variety of DNA lesions, including an abasic site, in efficiency (45). It may be possible that H_2O_2 induces lesions in DNA, for example an abasic site, which needs pol R1 to bypass it for mutagenesis. Collectively, our results suggest that H_2O_2 induces at least two types of lesions in DNA; one is oxidized pyrimidines that can be bypassed by endogenous *Salmonella* DNA polymerases for mutagenesis, and the other is abasic-site-like lesions that require the participation of pol R1 for mutagenesis.

The effect of visible light on chemical mutagenicity was observed for MB and NR. These chemicals have been reported to be more mutagenic in YG3001 than TA1535 (29). In this study, MB and NR, as well as B[*a*]P, exhibited higher mutagenicity in FPG-deficient strains than other strains, confirming the previous results. B[*a*]P usually requires metabolic activation to be mutagenic in *Salmonella*, but visible light activates it without metabolic activation (29). In the absence of irradiation, none of these chemicals was detectably mutagenic, even in YG3001 (data not shown). This observation is consistent with the proposed photodynamic generation of 8-OH-dG in DNA (46).

Our *nth* mutants exhibited a mild mutator phenotype, whereas the *nei* mutants had a spontaneous mutation frequency similar to wild-type cells. The *nth nei* double mutant, YG3206, exhibited a 20-fold increase in spontaneous mutation frequency (Fig. 3). This frequency is consistent with reports for analogous strains of *E. coli* (47,48). Considering the results shown above, L-cysteine and/or H_2O_2 may be candidates for increasing the spontaneous mutation frequency in YG3206. In addition, exposure to fluorescent light enhanced the mutation frequency. There may be certain endogenous chromophores that generate 8-OH-dG in DNA via photodynamic action.

Mammalian cells encode two Endo III-type glycosylases that recognize oxidative lesions. One of these, NTH1, removes a wide variety of oxidized pyrimidine derivatives, including thymine glycol and Fapy-dG (49–52). Knockout *Nth1* mice are reported to remain healthy (53,54). Three human genes, designated *NEIL1*, *NEIL2*, and *NEIL3*, encode proteins that contain sequence homologies to Endo VIII and FPG of *E. coli* (55–58). Inactivating mutations in *NEIL1* have been reported to correlate with human gastric cancer (59). In addition, RNA interference knockdown experiments in which a nearly 80% reduction in the *NEIL1* mRNA levels was achieved significantly sensitized cells to the killing effects of ionizing radiation (60). These data emphasize the importance of persistent oxidized pyrimidines in DNA. Taking into consideration the mutagenic effects of endogenous substances such as L-cysteine and H_2O_2, a possible critical role for *NEIL1* can be the exclusion of such endogenous mutagenic lesions, i.e., oxidized pyrimidines, for the long-term maintenance of genetic integrity.

In summary, we constructed a novel *S. typhimurium* strain, YG3206, by introducing *nth*$_{ST}$/*nei*$_{ST}$ deficiencies into the standard TA1535 Ames tester strain. The newly constructed strain exhibited higher specific sensitivity against chemicals that can be the cause of oxidized DNA pyrimidines. In particular, the strain detected the mutagenicity of naturally-occurring substances, such as L-cysteine, and suggested a possible involvement in spontaneous mutagenesis. We propose the combined use of YG3206 and YG3001 strains as a useful approach for mechanism-directed research of oxidative DNA damage.

Acknowledgements: The authors thank Dr. Peter Karran, Clare Hall Laboratories, Cancer Research, UK, London Research Institute, for critically reading the manuscript and his useful discussion. We also thank Drs. Toshihiro Ohta, Yukari Totsuka, and Kazuaki Kawai for generously providing precious chemicals. This work was supported in part by Grant-in-Aids for Cancer Research (19S-1) and for Scientific Research from the Ministry of Health, Labour, and Welfare of Japan.

References

1 Barnes DE, Lindahl T. Repair and genetic consequences of endogenous DNA base damage in mammalian cells. Annu Rev Genet. 2004; 38: 445–76.
2 Baute J, Depicker A. Base excision repair and its role in maintaining genome stability. Crit Rev Biochem Mol Biol. 2008; 43: 239–76.
3 Jackson AL, Chen R, Loeb LA. Induction of microsatellite instability by oxidative DNA damage. Proc Natl Acad

Sci USA. 1998; 95: 12468–73.
4 Ames BN, Shigenaga MK, Hagen TM. Oxidants, antioxidants, and the degenerative diseases of aging. Proc Natl Acad Sci USA. 1993; 90: 7915–22.
5 Cadet J, Douki T, Ravanat JL. Oxidatively generated damage to the guanine moiety of DNA: mechanistic aspects and formation in cells. Acc Chem Res. 2008; 41: 1075–83.
6 Friedberg EC, McDaniel LD, Schultz RA. The role of endogenous and exogenous DNA damage and mutagenesis. Curr Opin Genet Dev. 2004; 14: 5–10.
7 Dizdaroglu M. Oxidative damage to DNA in mammalian chromatin. Mutat Res. 1992; 275: 331–42.
8 Kasai H. Chemistry-based studies on oxidative DNA damage: formation, repair, and mutagenesis. Free Radic Biol Med. 2002; 33: 450–6.
9 Kasai H. Analysis of a form of oxidative DNA damage, 8-hydroxy-2′-deoxyguanosine, as a marker of cellular oxidative stress during carcinogenesis. Mutat Res. 1997; 387: 147–63.
10 Avkin S, Livneh Z. Efficiency, specificity and DNA polymerase-dependence of translesion replication across the oxidative DNA lesion 8-oxoguanine in human cells. Mutat Res. 2002; 510: 81–90.
11 Einolf HJ, Guengerich FP. Fidelity of nucleotide insertion at 8-oxo-7,8-dihydroguanine by mammalian DNA polymerase delta. Steady-state and pre-steady-state kinetic analysis. J Biol Chem. 2001; 276: 3764–71.
12 Haracska L, Prakash S, Prakash L. Yeast DNA polymerase zeta is an efficient extender of primer ends opposite from 7,8-dihydro-8-oxoguanine and O^6-methylguanine. Mol Cell Biol. 2003; 23: 1453–9.
13 Shibutani S, Takeshita M, Grollman AP. Insertion of specific bases during DNA synthesis past the oxidation-damaged base 8-oxodG. Nature. 1991; 349: 431–4.
14 Fowler RG, White SJ, Koyama C, Moore SC, Dunn RL, Schaaper RM. Interactions among the *Escherichia coli mutT*, *mutM*, and *mutY* damage prevention pathways. DNA Repair (Amst). 2003; 2: 159–73.
15 Boiteux S, Gajewski E, Laval J, Dizdaroglu M. Substrate specificity of the *Escherichia coli* Fpg protein (formamidopyrimidine-DNA glycosylase): excision of purine lesions in DNA produced by ionizing radiation or photosensitization. Biochemistry. 1992; 31: 106–10.
16 Michaels ML, Pham L, Cruz C, Miller JH. MutM, a protein that prevents G C→T A transversions, is formamidopyrimidine-DNA glycosylase. Nucleic Acids Res. 1991; 19: 3629–32.
17 Kreutzer DA, Essigmann JM. Oxidized, deaminated cytosines are a source of C→T transitions in vivo. Proc Natl Acad Sci USA. 1998; 95: 3578–82.
18 Shen JC, Rideout WM, III, Jones PA. The rate of hydrolytic deamination of 5-methylcytosine in double-stranded DNA. Nucleic Acids Res. 1994; 22: 972–6.
19 Jones PA, Rideout WM, III, Shen JC, Spruck CH, Tsai YC. Methylation, mutation and cancer. Bioessays. 1992; 14: 33–6.
20 Krokan HE, Nilsen H, Skorpen F, Otterlei M, Slupphaug G. Base excision repair of DNA in mammalian cells. FEBS Lett. 2000; 476: 73–7.
21 Melamede RJ, Hatahet Z, Kow YW, Ide H, Wallace SS. Isolation and characterization of endonuclease VIII from *Escherichia coli*. Biochemistry. 1994; 33: 1255–64.
22 Hatahet Z, Kow YW, Purmal AA, Cunningham RP, Wallace SS. New substrates for old enzymes. 5-Hydroxy-2′-deoxycytidine and 5-hydroxy-2′-deoxyuridine are substrates for *Escherichia coli* endonuclease III and formamidopyrimidine DNA *N*-glycosylase, while 5-hydroxy-2′-deoxyuridine is a substrate for uracil DNA *N*-glycosylase. J Biol Chem. 1994; 269: 18814–20.
23 Demple B, Harrison L. Repair of oxidative damage to DNA: enzymology and biology. Annu Rev Biochem. 1994; 63: 915–48.
24 Lindahl T. Repair of intrinsic DNA lesions. Mutat Res. 1990; 238: 305–11.
25 Wallace SS. DNA damages processed by base excision repair: biological consequences. Int J Radiat Biol. 1994; 66: 579–89.
26 Evans J, Maccabee M, Hatahet Z, Courcelle J, Bockrath R, Ide H, *et al.* Thymine ring saturation and fragmentation products: lesion bypass, misinsertion and implications for mutagenesis. Mutat Res. 1993; 299: 147–56.
27 Feig DI, Sowers LC, Loeb LA. Reverse chemical mutagenesis: identification of the mutagenic lesions resulting from reactive oxygen species-mediated damage to DNA. Proc Natl Acad Sci USA. 1994; 91: 6609–13.
28 Purmal AA, Kow YW, Wallace SS. Major oxidative products of cytosine, 5-hydroxycytosine and 5-hydroxyuracil, exhibit sequence context-dependent mispairing in vitro. Nucleic Acids Res. 1994; 22: 72–8.
29 Suzuki M, Matsui K, Yamada M, Kasai H, Sofuni T, Nohmi T. Construction of mutants of *Salmonella typhimurium* deficient in 8-hydroxyguanine DNA glycosylase and their sensitivities to oxidative mutagens and nitro compounds. Mutat Res. 1997; 393: 233–46.
30 Martínez A, Urios A, Blanco M. Mutagenicity of 80 chemicals in *Escherichia coli* tester strains IC203, deficient in OxyR, and its *oxyR*$^+$ parent WP2 *uvrA*/pKM101: detection of 31 oxidative mutagens. Mutat Res. 2000; 467: 41–53.
31 Levin DE, Hollstein M, Christman MF, Schwiers EA, Ames BN. A new Salmonella tester strain (TA102) with A X T base pairs at the site of mutation detects oxidative mutagens. Proc Natl Acad Sci USA. 1982; 79: 7445–9.
32 Maron DM, Ames BN. Revised methods for the Salmonella mutagenicity test. Mutat Res. 1983; 113: 173–215.
33 Link AJ, Phillips D, Church GM. Methods for generating precise deletions and insertions in the genome of wild-type *Escherichia coli*: application to open reading frame characterization. J Bacteriol. 1997; 179: 6228–37.
34 Yamada M, Hakura A, Sofuni T, Nohmi T. New method for gene disruption in *Salmonella typhimurium*: construction and characterization of an *ada*-deletion derivative of *Salmonella typhimurium* TA1535. J Bacteriol. 1993; 175: 5539–47.
35 Katafuchi A, Nakano T, Masaoka A, Terato H, Iwai S, Hanaoka F, *et al.* Differential specificity of human and

Escherichia coli endonuclease III and VIII homologues for oxidative base lesions. J Biol Chem. 2004; 279: 14464-71.
36 Josephy PD, Gruz P, Nohmi T. Recent advances in the construction of bacterial genotoxicity assays. Mutat Res. 1997; 386: 1-23.
37 Nohmi T. Novel DNA polymerases and novel genotoxicity assays. Genes Environ. 2007; 29: 75-88.
38 Yamada M, Sedgwick B, Sofuni T, Nohmi T. Construction and characterization of mutants of *Salmonella typhimurium* deficient in DNA repair of O^6-methylguanine. J Bacteriol. 1995; 177: 1511-9.
39 Ishikawa S, Mochizuki M. Mutagenicity and cross-linking activity of chloroalkylnitrosamines, possible new antitumor lead compounds. Mutagenesis. 2003; 18: 331-5.
40 Okochi E, Namai E, Ito K, Mochizuki M. Activation of *N*-nitrosodialkylamines to mutagens by a metalloporphyrin/oxidant model system for cytochrome P450. Biol Pharm Bull. 1995; 18: 49-52.
41 Yamada M, Matsui K, Nohmi T. Development of a bacterial hyper-sensitive tester strain for specific detection of the genotoxicity of polycyclic aromatic hydrocarbons. Genes Environ. 2006; 28: 23-30.
42 Glatt H. Mutagenicity spectra in *Salmonella typhimurium* strains of glutathione, L-cysteine and active oxygen species. Mutagenesis. 1989; 4: 221-7.
43 Stark AA, Pagano DA, Glass G, Kamin-Belsky N, Zeiger E. The effects of antioxidants and enzymes involved in glutathione metabolism on mutagenesis by glutathione and L-cysteine. Mutat Res. 1994; 308: 215-22.
44 Glatt H, Protic-SabljiC M, Oesch F. Mutagenicity of glutathione and cysteine in the Ames test. Science. 1983; 220: 961-3.
45 Goldsmith M, Sarov-Blat L, Livneh Z. Plasmid-encoded MucB protein is a DNA polymerase (pol RI) specialized for lesion bypass in the presence of MucA′, RecA, and SSB. Proc Natl Acad Sci USA. 2000; 97: 11227-31.
46 Kim SR, Kokubo K, Matsui K, Yamada N, Kanke Y, Fukuoka M, *et al.* Light-dependent mutagenesis by benzo[*a*]pyrene is mediated via oxidative DNA damage. Environ Mol Mutagen. 2005; 46: 141-9.
47 Jiang D, Hatahet Z, Blaisdell JO, Melamede RJ, Wallace SS. *Escherichia coli* endonuclease VIII: cloning, sequencing, and overexpression of the nei structural gene and characterization of *nei* and *nei nth* mutants. J Bacteriol. 1997; 179: 3773-82.
48 Saito Y, Uraki F, Nakajima S, Asaeda A, Ono K, Kubo K, *et al.* Characterization of endonuclease III (*nth*) and endonuclease VIII (*nei*) mutants of *Escherichia coli* K-12. J Bacteriol. 1997; 179: 3783-5.
49 Asagoshi K, Odawara H, Nakano H, Miyano T, Terato H, Ohyama Y, *et al.* Comparison of substrate specificities of *Escherichia coli* endonuclease III and its mouse homologue (mNTH1) using defined oligonucleotide substrates. Biochemistry. 2000; 39: 11389-98.
50 Dizdaroglu M, Karahalil B, Senturker S, Buckley TJ, Roldan-Arjona T. Excision of products of oxidative DNA base damage by human NTH1 protein. Biochemistry. 1999; 38: 243-6.
51 Aspinwall R, Rothwell DG, Roldan-Arjona T, Anselmino C, Ward CJ, Cheadle JP, *et al.* Cloning and characterization of a functional human homolog of *Escherichia coli* endonuclease III. Proc Natl Acad Sci USA. 1997; 94: 109-14.
52 Hilbert TP, Boorstein RJ, Kung HC, Bolton PH, Xing D, Cunningham RP, *et al.* Purification of a mammalian homologue of *Escherichia coli* endonuclease III: identification of a bovine pyrimidine hydrate-thymine glycol DNAse/AP lyase by irreversible cross linking to a thymine glycol-containing oligoxynucleotide. Biochemistry. 1996; 35: 2505-11.
53 Ocampo MT, Chaung W, Marenstein DR, Chan MK, Altamirano A, Basu AK, *et al.* Targeted deletion of *mNth1* reveals a novel DNA repair enzyme activity. Mol Cell Biol. 2002; 22: 6111-21.
54 Takao M, Kanno S, Shiromoto T, Hasegawa R, Ide H, Ikeda S, *et al.* Novel nuclear and mitochondrial glycosylases revealed by disruption of the mouse *Nth1* gene encoding an endonuclease III homolog for repair of thymine glycols. EMBO J. 2002; 21: 3486-93.
55 Bandaru V, Sunkara S, Wallace SS, Bond JP. A novel human DNA glycosylase that removes oxidative DNA damage and is homologous to *Escherichia coli* endonuclease VIII. DNA Repair (Amst). 2002; 1: 517-29.
56 Hazra TK, Izumi T, Boldogh I, Imhoff B, Kow YW, Jaruga P, *et al.* Identification and characterization of a human DNA glycosylase for repair of modified bases in oxidatively damaged DNA. Proc Natl Acad Sci USA. 2002; 99: 3523-8.
57 Morland I, Rolseth V, Luna L, Rognes T, Bjoras M, Seeberg E. Human DNA glycosylases of the bacterial Fpg/MutM superfamily: an alternative pathway for the repair of 8-oxoguanine and other oxidation products in DNA. Nucleic Acids Res. 2002; 30: 4926-36.
58 Takao M, Kanno S, Kobayashi K, Zhang QM, Yonei S, van der Horst GT, *et al.* A back-up glycosylase in *Nth1* knock-out mice is a functional Nei (endonuclease VIII) homologue. J Biol Chem. 2002; 277: 42205-13.
59 Shinmura K, Tao H, Goto M, Igarashi H, Taniguchi T, Maekawa M, *et al.* Inactivating mutations of the human base excision repair gene *NEIL1* in gastric cancer. Carcinogenesis. 2004; 25: 2311-7.
60 Rosenquist TA, Zaika E, Fernandes AS, Zharkov DO, Miller H, Grollman AP. The novel DNA glycosylase, NEIL1, protects mammalian cells from radiation-mediated cell death. DNA Repair (Amst). 2003; 2: 581-91.

COMMENTARY

液体クロマトグラフィータンデム質量分析法を用いたDNA損傷研究法

Quantification of DNA Adducts by Using Liquid Chromatography/Tandem Mass Spectrometry

松田知成[1]*・永吉晴奈[2]・椙村春彦[3]・周　佩欣[4]
Tomonari MATSUDA,[1]* Haruna NAGAYOSHI,[2]
Haruhiko SUGIMURA,[3] and Pei-Hsin CHOU[4]

[1] 京都大学大学院工学研究科附属流域圏総合環境質研究センター　*Research Center for Environmental Quality Management, Kyoto University, Otsu, SHIGA, JAPAN*
[2] 大阪府公衆衛生研究所　*Osaka Prefectural Institute of Public Health, Osaka, JAPAN*
[3] 浜松医科大学　*Hamamatsu University School of Medicine, Hamamatsu, JAPAN*
[4] 国立成功大学　*National Cheng Kung University, Tainan, TAIWAN*

Formation of DNA adducts is a crucial step for carcinogenesis and aging. However, until recently, it was difficult to quantify trace amount of DNA adducts in living organisms. Development of liquid chromatography/tandem mass spectrometry (LC/MS/MS) equipments enables us to quantify DNA adducts at practical sensitivity. Molecular epidemiological study such as aldehyde dehydrogenase 2 gene (*ALDH2*) genotypes and risk of alcohol-related DNA damage has been conducted by using LC/MS/MS. Furthermore, we developed "DNA adductome" analysis which can display comprehensive picture of DNA adducts in living organisms. These techniques may contribute to understand mechanisms of carcinogenesis and aging.

(Received April 27, 2009; Accepted June 8, 2009)

1. DNA付加体とは

DNA付加体とは，外来の発がん物質や生体内で生じる反応性に富む化学種が，DNAと共有結合したものである．DNAはアデニン，グアニン，チミン，シトシン，および5メチルシトシンの5種類の塩基，デオキシリボース，そしてリン酸からなる高分子である．化学物質はこのうちどの部分も攻撃しうるが，塩基部分への付加体について特によく研究されている．本稿においてはDNA塩基部分への付加体の意味で，「DNA付加体」という言葉を使用する．

ある種のDNA付加体は，細胞分裂の際DNA合成を阻害し，細胞死や突然変異を誘発する．この結果，DNA付加体は突然変異，発がん，加齢に密接に関連すると考えられている．数多くのDNA付加体についてその突然変異への寄与，DNA修復されやすさなどが調べられているものの，DNA付加体の種類は多種多様であり，生体内の付加体について全容が明らかになっているわけではない．

2. DNA付加体のさまざまな測定法

生体に対するDNA付加体の影響を調べるため，付加体の検出が試みられてきたが，微量なDNA付加体を検出・定量することは，最近まで非常に困難であった．^{32}P-ポストラベル法はDNA付加体の分析に最もよく使われてきた方法である．ヌクレアーゼP1法やブタノール抽出法，非変性poly-acrylamide gel electrophoresis (PAGE)分離法などの変法も開発され，分子量の大きな化合物の付加体（例えば代表的な発がん物質ベンゾ[*a*]ピレンの付加体など）については非常に感度よく定量できる[1]．しかし，低分子量の付加体（例えば水酸基やメチル基が付いただけのものなど）をこの方法で解析することは極めて困難であった．

ガスクロマトグラフ質量分析計や液体クロマトグラフ質量分析計を使う方法も有望である．これらの分析機器を用いれば，数種類のDNA付加体を同時に定量的に測定できる．ガスクロマトグラフを用いる場合はDNAを加水分解

本稿は第35回BMSコンファレンスでの講演内容を著したものです．

* Correspondence to: Tomonari MATSUDA, *Research Center for Environmental Quality Management, Kyoto University, 1-2 Yumihama, Otsu, Shiga 520-0811, JAPAN*, e-mail: matsuda@z05.mbox.media.kyoto-u.ac.jp
松田知成，京都大学大学院工学研究科附属流域圏総合環境質研究センター，〒520-0811 大津市由美浜1-2

して塩基部分を測定する．一方，液体クロマトグラフは，酵素でデオキシヌクレオシドに分解して測定するのが一般的である．これらの中で液体クロマトグラフィータンデム質量分析法 (liquid chromatography/tandem mass spectrometry: LC/MS/MS) は，デオキシヌクレオシドを最も感度よく測定できる機器である．LC/MS/MS を用いて DNA 付加体を測定する試みは今までにいくつかあったが，一世代前の LC/MS/MS を用いたこれらの研究では，少量の DNA サンプルから DNA 付加体を測定するには感度が不十分であった．しかし最新型の LC/MS/MS を用いれば，5 μg の DNA からでも 10^8 塩基当たり数個の DNA 付加体が定量可能で，検出だけなら，10^9 塩基当たり数個のレベルまで到達していることを筆者は確認した[2]．これは，^{32}P-ポストラベル法に迫る感度である．また，LC/MS/MS の分析では 10 種類以上のイオンの質量を，感度を落とすことなく同時にモニターでき，複数の DNA 付加体を同時に定量可能であるという利点もある．簡便性，定量性，再現性では LC/MS/MS は ^{32}P-ポストラベル法を凌駕している．DNA 付加体の分析法は早晩 LC/MS/MS が主流になるだろう．

3. LC/MS/MS による DNA 付加体の分析法

まず，臓器や培養細胞などの生体サンプルから DNA を抽出する．きれいに精製できればどのような方法でも良いと思うが，測定する付加体の種類によっては特別な精製法が必要である．例えば，酸化的 DNA 損傷 8-oxo-dG を測定する際は DNA 抽出の過程で自然に生成しやすいので，DNA 抽出に使用する緩衝液に酸化を抑制する試薬を加える．また，後述するアセトアルデヒドの DNA 付加体を測定する際には，DNA 抽出過程でエタノール沈殿の代わりにイソプロパノール沈殿を行ったりする（エタノールに不純物としてアセトアルデヒドが含まれるため）．

DNA が精製できたら次は DNA を酵素で分解し，デオキシヌクレオシド体にする．これもいくつかの方法があるが，われわれは Micrococcus Nuclease, Spleen phosphodiesterase II，およびアルカリフォスファターゼという 3 種類の酵素を用いている．

次はいよいよ LC/MS/MS の測定である．Fig. 1 に例として N^2-ethyl-dG という DNA 付加体の開裂パターンを示す．付加体デオキシヌクレオシドの多くはエレクトロスプレーイオン化法により，プロトンが 1 個付加した正イオン（プロトン付加分子）を生じる．このイオンが衝突セルに導入されると，多くの場合，デオキシリボースと塩基間のグリコシド結合が開裂し，塩基部分の質量＋1 のプロダクト（フラグメント）イオンを生じる．デオキシリボース部分の質量は 116 なので，塩基部分の質量は必ずデオキシヌクレオシドの質量－116 になる．したがって，デオキシヌクレオシドの質量を M としたとき，プリカーサーイオンを M＋1，プロダクトイオンを (M－116)＋1 に設定して，multiple reaction monitoring (MRM) スキャンを行うと，ほとんどの場合うまく DNA 付加体を測定することができる．

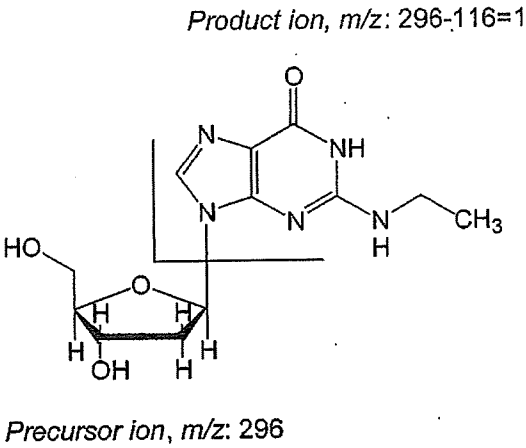

Fig. 1. Degradation pattern of DNA adducts in LC/MS/MS analysis. This figure shows the structure of N^2-ethyl-dG as an example of DNA adducts. In many cases, the glycoside bond, which links deoxyribose and DNA base, is easily broken in CID (collision-induced dissociation) cell.

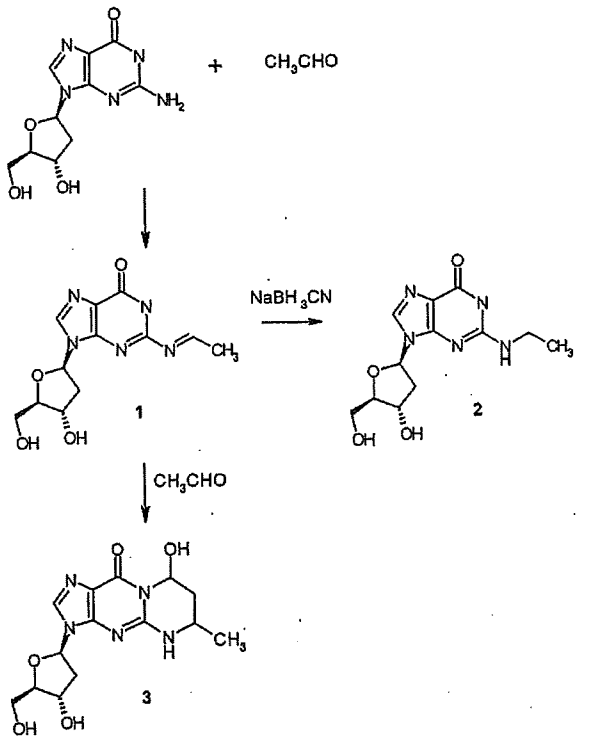

Fig. 2. Formation of acetaldehyde-dG adducts. 1: N^2-ethylidene-dG, 2: N^2-ethyl-dG, 3: α-Me-γ- OH-PdG

4. DNA 付加体の測定例

筆者らはこのような方法でさまざまな DNA 付加体の定量を行っているが，次にその一例を示したい．読者の中にはお酒が好きな人も多いと思うが，お酒を飲むとすぐ赤くなる人（専門用語でフラッシャーという）は，飲酒による食道がんのリスクが非常に高くなる[3]．エタノールは体内で酸化されて反応性の高いアセトアルデヒドになる．アセトアルデヒドはアルデヒド脱水素酵素 (aldehyde dehydrogenase 2: ALDH2) によって酢酸へと無毒化されるが，

Table 1. Acetaldehyde-derived DNA Adducts in *ALDH2*-deficient Alcoholics[4]

Acetaldehyde-derived DNA adducts	*ALDH2* Genotype		*p*-Value
	(*1/*1) [n=19] (Normal type)	(*1/*2) [n=25] (Deficient type)	
N^2-Ethyl-dG	17.8±15.9	130±52	0.03
α-S-Me-γ-OH-PdG	42.9±6.0	92.4±12.9	0.01
α-R-Me-γ-OH-PdG	61.3±6.4	114±15	0.02

Values are means±standard error of the mean (fmol/μM dG).
p-Values were calculated by the Wilcoxon–Mann–Whitney test (N^2-ethyl-dG) and *t*-test (α-Me-γ-OH-PdG).

Table 2. Stomach DNA Adduct Levels in Control and Alcohol-treated Mice Having Different *Aldh2* Genotypes[5]

	Aldh2 Genotype	n	N^2-Ethylidene dG level (adducts/10^7 bases)
Water	+/+	5	3.1±2.3
	+/−	6	2.0±0.6
	−/−	5	2.2±0.4
20% Ethanol	+/+	6	4.8±2.6
	+/−	5	7.9±1.1
	−/−	4	48.6±12.0

Values are means±standard error of the mean.
Mice were fed with water or 20% ethanol for 5 weeks.

日本人の約半数はこの酵素が欠損していて，体内にアセトアルデヒドが蓄積しやすい．アセトアルデヒドはDNA損傷性や突然変異原性をもつ化合物なので，フラッシャー，すなわち *ALDH2* 欠損者では DNA 損傷が蓄積した結果，がんのリスクが高くなるのではないかと考えられてきた．アセトアルデヒドにより生成する DNA 付加体の構造を Fig. 2 に示す．久里浜病院の横山　顕先生の協力を得てアルコール依存症患者の血液中 DNA の分析を行ったところ，Table 1 に示すように *ALDH2* 欠損者に DNA 付加体が蓄積していることが明らかになった[4]．また，Table 2 は正常マウスおよび *Aldh2* ノックアウトマウスに 20% エタノールを5週間与えたときの，胃中の DNA 付加体（N^2-ethylidine-dG，還元して N^2-ethyl-dG として測定）を定量したものである．*Aldh2* +/+ は正常型，+/− はヘテロ欠損型，−/− はホモ欠損型である．飲酒したマウスでは，水を与えたマウスに比べて DNA 付加体が増えており，さらに *Aldh2* の遺伝子多型によって付加体数が劇的に変わっているのがわかる[5]．つまり，お酒の弱い人は，お酒を飲むと胃の DNA にダメージを受けやすいことがわかる．

5. DNA アダクトーム解析—生体内には何種類くらいの DNA 付加体が存在するのか？—

筆者は LC/MS/MS を用いて，既知 DNA 付加体の定量解析をするだけではなく，生体内の DNA 付加体を網羅的に解析する手法を開発してきた．この方法をプロテオームやメタボロームをもじって「DNA アダクトーム解析」と命名した[6,7]．DNA 付加体を質量分析により定量する場合，プリカーサーイオンとプロダクトイオンの質量差を 116 にするとうまく測定できることはすでに述べたが，プリカーサーイオンとプロダクトイオンの質量差を常に 116 に保ちながら，さまざまな質量について網羅的に解析することにより，未知の DNA 付加体を検出できる．現在われわれは感度の問題から，MRM モードを利用している．使用している LC/MS/MS (Waters-Micromass 社製，Quattro Pt) では，一度に最大 32 チャンネルの分析が可能なので，例えば同じサンプルを 15 回に分けて分析すれば，質量 266 から 629 の範囲について調べることができる (Fig.

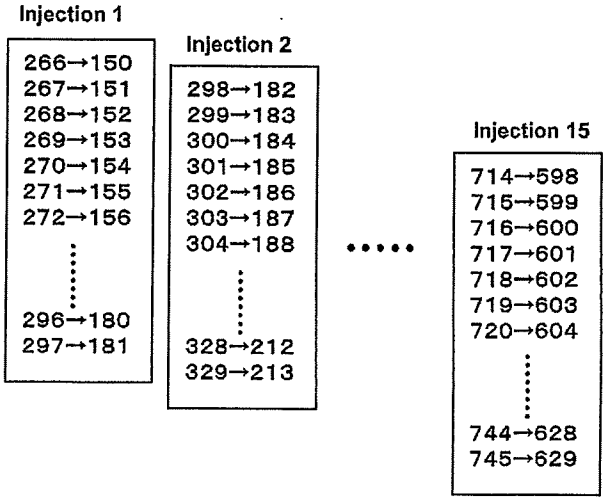

Fig. 3. An example of parameter-setting of precursor ion and product ion in DNA adductome analysis. Note that the difference of m/z between precursor ion and product ion is always 116.

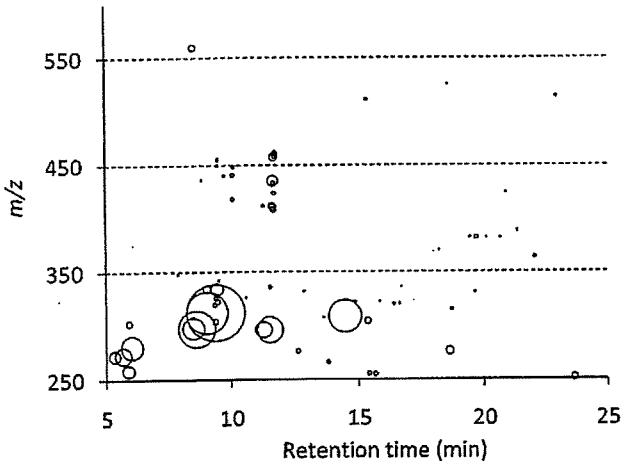

Fig. 4. An example of adductome map of human colon DNA. The horizontal axis is retention time of LC/MS/MS and the vertical axis is *m/z*. The size of the babble represent the area of detected peaks.

3). 今後技術革新により質量分析計の感度が上がればニュートラルロススキャンを使って，一度の分析で同じことができるようになるだろう．

Fig. 4 は，ヒトの大腸の DNA について，DNA アダクトーム解析した例である．出現したピーク（おそらく DNA 付加体由来）の面積をバブル図にプロットしている．質量分析では測定物質の構造によりイオン化の効率が異なるため，面積の大きなピークが必ずしも量が多い付加体に対応しているわけではないが，DNA アダクトーム解析により生体内に LC/MS/MS で検出可能な DNA 付加体が何種類ぐらいあり，その質量はどのくらいかという情報が得られる．われわれは，さまざまな DNA サンプルについてこの解析を進めており，重要な未知の DNA 付加体の構造決定を試みている．

6. おわりに

本稿では DNA 付加体の定量分析の分野では LC/MS/MS がすでに実用段階に入っており，主流になりつつあること，および，DNA アダクトームという方法を用いることにより，生物の臓器中に存在する未知の DNA 付加体の網羅的解析ができるということを紹介してきた．LC/MS/MS の技術革新に伴う感度や分解能の向上は目覚ましく，今後ますます簡便に，より網羅的に DNA 付加体が解析できるようになるだろう．これにより DNA 付加体の全容が明らかになれば，発がんや老化のメカニズム解明に役立つだろう．

謝　辞　本稿の発表の機会を与えていただいた，BMS コンファレンス実行委員の皆様に深く感謝いたします．なお，本稿で発表した内容は，NEDO (The New Energy and Industrial Technology Development Organization) 産業技術研究助成事業，日本学術振興会科学研究費補助金，厚生労働がん研究費により行った．

文　献

1) I. Terashima, N. Suzuki, and S. Shibutani, *Chem. Res. Toxicol.*, **15**, 305 (2002).
2) 松田知成，環境変異原研究，**26**, 199 (2004).
3) P. J. Brooks, *et al.*, *PLoS Medicine*, **6**, 258 (2009).
4) T. Matsuda, H. Yabushita, R. Kanaly, S. Shibutani, and A. Yokoyama, *Chem. Res. Toxicol.*, **19**, 1374 (2006).
5) H. Nagayoshi, *et al.*, *Mutat. Res.*, **673**, 74 (2009).
6) R. A. Kanaly, *et al.*, *Antioxidants & Redox Signaling*, **8**, 993 (2006).
7) R. Kanaly, S. Matsui, T. Hanaoka, and T. Matsuda, *Mutat. Res.*, **625**, 83 (2007).

Keywords: DNA adduct, LC/MS/MS, DNA adductome

3. アダクトミクス
—DNAおよびタンパク質付加体の網羅的解析

松田知成，足立　淳，周　佩欣

DNAやタンパク質などの生体高分子は常に活性酸素や過酸化脂質に攻撃されている．脂質過酸化で生じる反応性の高いアルデヒドなどはこれら生体高分子に付加体を形成する．さまざまな付加体を網羅的に検出し，データベースを整備し，それらの生物学的意義を明らかにしようとする研究を総称して「アダクトミクス」と呼ぶ．アダクトミクス研究はまだ始まったばかりであるが，近年の分析技術の革新により今後発展が期待される．本稿では，われわれの研究室で開発した「DNAアダクトーム法」と，タンパク質のレドックス修飾を定量的に検出する「DLIAA法」について解説する．

はじめに

活性酸素や過酸化脂質は細胞内のDNAやタンパク質などの生体高分子を攻撃し損傷を与える．特に反応性の高い化学物質が生体高分子に共有結合してしまうことを付加体形成と呼んでいる．生体高分子に付加体が蓄積すると，その本来の機能が変化したり失われたりすることは容易に推測できる．その結果，発癌をはじめとするさまざまな疾患を誘発することが懸念されている．例えば，DNA付加体が蓄積するとDNA複製の際，付加体の手前でDNA合成が停止し，アポトーシスまたは突然変異を誘発し，老化や発癌の原因になると考えられている．

近年，質量分析器の性能が向上し，生体内の微量なDNA付加体やタンパク質付加体を定量できるようになってきた．そこで，さまざまな付加体を網羅的に検出し，データベースを整備し，それらの生物学的意義を明らかにしようとする研究を総称して「アダクトミクス」と呼ぶことを提案したい．アダクトミクス研究はまだ始まったばかりであるが，近年の分析技術の革新により今後発展が期待される．われわれの研究室では，DNA付加体を網羅的に検出する「DNAアダクトーム法」を開発してきた．そこで，この稿ではこの方法の原理やプロトコールについて詳しく解説したい．一方，タンパク質付加体についての網羅的解析法はまだ開発されていないが，タンパク質のシステイン残基

[キーワード&略語]
アダクトミクス，DNAアダクトーム，DLIAA法

DLIAA：double labeling approach using isotope amino acids and affinity tags
ICAT：isotope coded affinity tags
LC-MS/MS：liquid chromatograph tandem mass spectrometry
（液体クロマトグラフタンデム質量分析器）
Prx6：peroxiredoxin 6（ペルオキシレドキシン6）
SILAC：stable isotope labeling with amino acids in cell culture

Adductomics—Comprehensive analysis of DNA adducts and protein adducts
Tomonari Matsuda[1]/Jun Adachi[2]/Pei-Hsin Chou[3]：Research Center for Environmental Quality Management, Kyoto University[1]/Kyoto Sustainability Initiative, Graduate School of Global Environmental Studies, Kyoto University[2]/Department of Environmental Engineering, National Cheng Kung University, Taiwan[3]（京都大学工学研究科附属流域圏総合環境質研究センター[1]/京都大学地球環境学堂京都サステイナビリティ・イニシアティブ[2]/國立成功大学環境工程学系，台湾[3]）

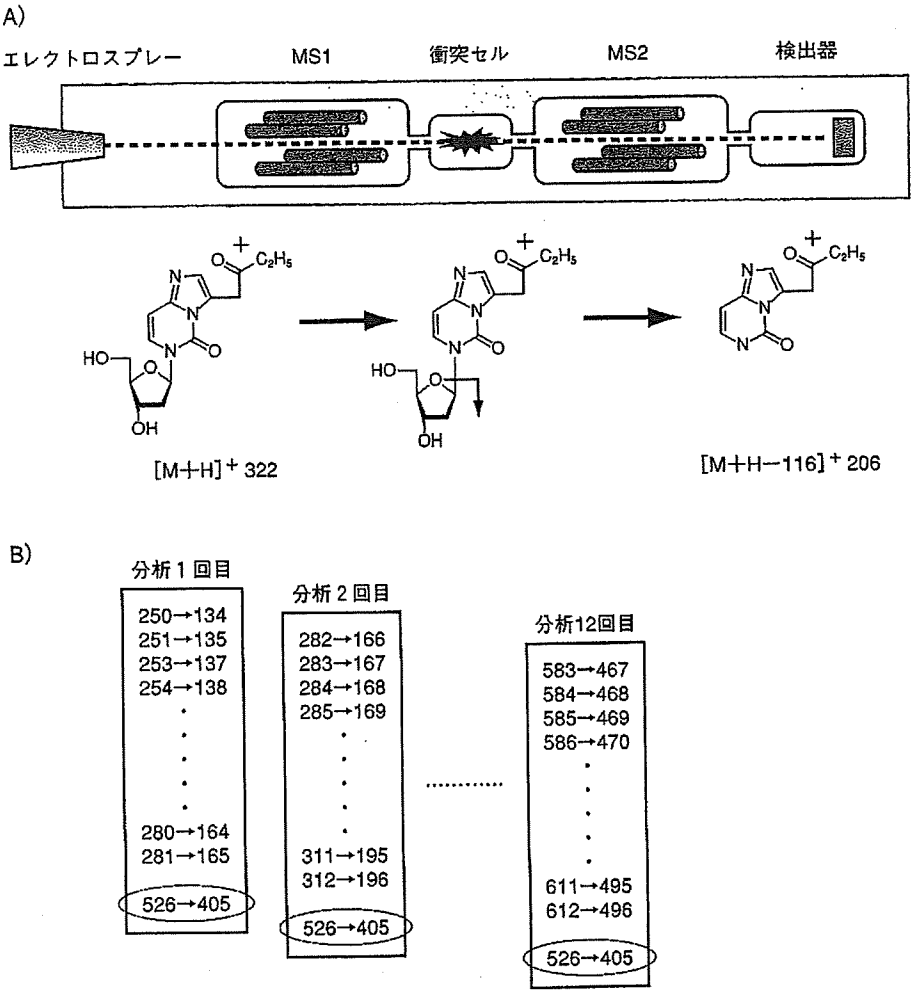

図2　DNAアダクトーム法の原理

A）デオキシヌクレオシドをLC-MS/MSで分析する際，衝突セルで容易にグリコシド結合が開裂する．図中央に，例として4-OHE-dCというDNA付加体の開裂パターンを示す．この化合物の分子量は321である．エレクトロスプレーでイオン化されると，プロトンが1個付加した陽イオンが生成する．このイオンの質量は321＋1＝322，電荷は＋1なので，*m/z* 値は322である．このイオンをMS1で選択的に通過させ，衝突セルに導入する．衝突セルでグリコシド結合が壊されると，デオキシリボースの質量116を失った，*m/z* 206の陽イオンが生成する．これをMS2で選択的に検出器まで通して検出する．B）DNAアダクトームでは，親イオンと娘イオンの質量差を116に保ちつつ，*m/z*値を1刻みにしらみつぶしに分析する．同じサンプルについて12回分析を繰り返すと，*m/z* 250から612まで網羅的に調べることができる．丸をつけた526→405は，われわれが使っている内部標準をモニターするための設定である．なお，分析1回目の252→136はdAの*m/z*でシグナルが強すぎるのでモニターしない

を同時測定する）．ここで*m/z*とは，イオンの質量を電荷で割った値である．対応する娘イオンは，（親イオンの*m/z*値）－116になるように設定する（すなわち，*m/z* 134から*m/z* 165まで）．また，内部標準も同時にモニターする．1回の分析で30セットの質量しかモニターしない理由は，機械の性能上それ以上の同時測定が難しいからである．2回目の分析では，親イオン→娘イオンの設定値を*m/z* 282→166から*m/z* 312→196および内部標準のモニター，3回目の分析では，*m/z* 313→197から*m/z* 342→226および内部標準のモニター，のようにしらみつぶしに分析し，同じサンプルについて合計12回，*m/z* 250から612までの範囲について解析する（図2）．この分析により得られたピークは，DNA付加体由来である可能性が高い．

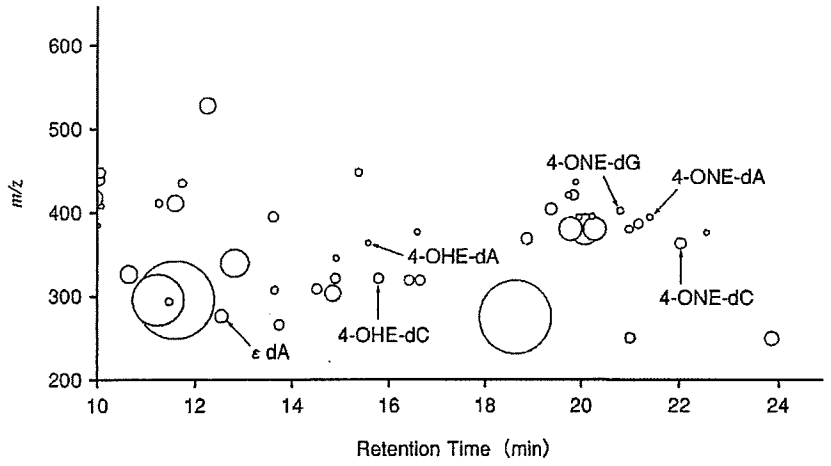

図3　DNAアダクトームマップ
病気で亡くなったヒトの脾臓DNAをDNAアダクトーム解析した例．図1で示したいくつかのDNA付加体ピークが検出されている

分析に用いたDNA量と，内部標準のピーク面積で，DNA付加体ピークの面積を補正し，下記のアダクトームマップにプロットする．

3）DNAアダクトームの解析例

図3に，アダクトームマップの一例を示す．剖検例のヒト脾臓からDNAを精製しDNAアダクトーム解析を行った（論文投稿準備中；なお，本研究にあたっては遺族のインフォームドコンセント，および共同研究者を含む所属大学において倫理委員会の承認を得ている）．横軸はHPLCの保持時間，縦軸は検出されたピークのm/z，バブルの大きさは補正したピーク面積に比例している．DNA付加体由来と思われるたくさんのピークが検出されたが，そのうちのいくつかのピークは，保持時間とm/zの値から図1で示した，4-ONE-dC，4-ONE-dA，4-ONE-dG，4-OHE-dC，4-OHE-dAなどであると同定することができた．

このように，DNAアダクトーム法は既知，および未知のDNA付加体を網羅的に解析し，その全体像をつかむのに優れた方法である．現在この方法を用いて，ヒト組織中の新規DNA付加体の構造決定などの基礎研究を行うとともに，新規の遺伝毒性試験として応用を試みている．

2 タンパク質のシステイン酸化修飾変化を定量的に検出するDLIAA法

活性酸素種はタンパク質も酸化修飾するが，なかでもシステインのチオール基はその反応性の高さから，還元型（-SH），チオールラジカル（-S・），ジスルフィド（Cys-S-S-Cys），スルフェン酸（-SOH），スルフィン酸（$-SO_2H$），スルフォン酸（$-SO_3H$），ニトロシル化（-S-NO）の形態をとることが知られている．システインと過酸化水素との反応には選択性があることも報告されているが[7]，細胞内での標的となるシステインやその酸化形態，酸化修飾の動態変化については不明な部分が多い．そこで酸化ストレスによるシステインの修飾変化を定量するために，DLIAA（double labeling approach using isotope amino acids and affinity tags）法というプロテオームレベルのシステイン酸化修飾の定量法を開発してきた．本法の鍵となる技術は，ICAT（isotope coded affinity tags）による還元型・酸化型システインの2段階標識とSILAC（stable isotope labeling with amino acids in cell culture）法による定量である．

標準的なショットガン式プロテオーム解析方法では，タンパク質をDTTなどの還元剤で還元したのち，アルキル化，トリプシン消化して，ナノLC-MS/MSで同定・定量を行う．その際，スルフェン酸，ジスルフィド，ニトロシル基などの可逆的なシステイン酸化修飾は，DTTによって還元されるため，元から還元されていたシステイン（-SH）と区別がつかなくなってしまう．そこで，質量の異なるICATタグ（^{12}C体と^{13}C体）を還元型・可逆的酸化型システインにそれぞ

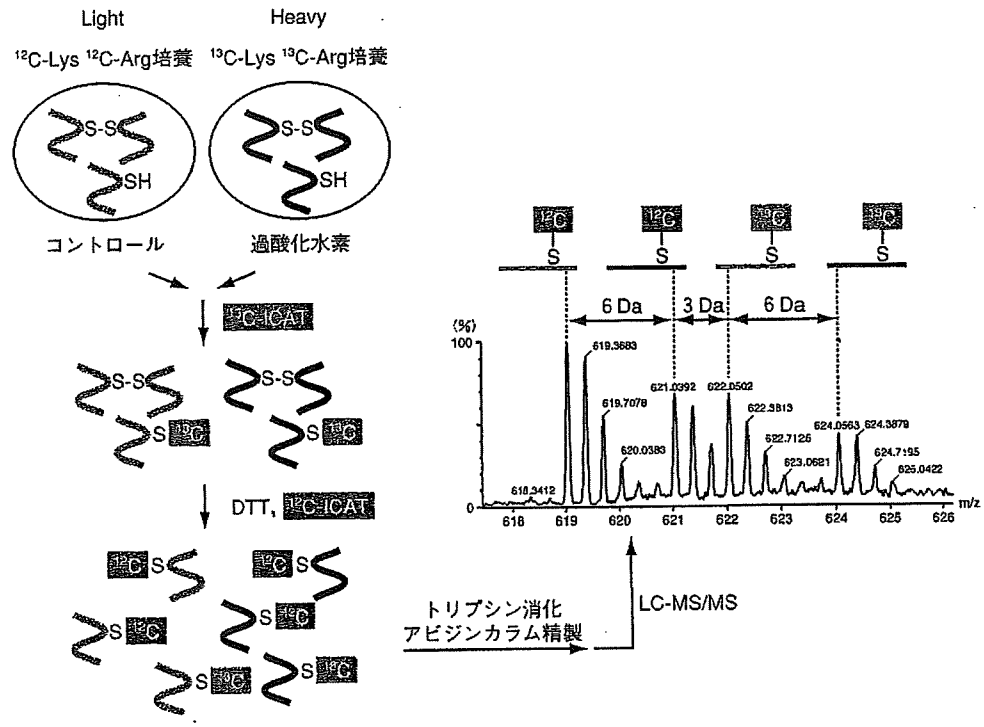

図4　DLIAA法の原理
SILAC法で標識した「軽い」細胞と「重い」細胞のどちらか一方に被検物質を曝露後，混合する．試料中のタンパク質の還元型システイン（-SH）を^{13}C体ICATタグで標識する（1段階目の標識）．還元剤で可逆的酸化型システインを還元し，^{12}C体ICATタグで標識する（2段階目の標識）．トリプシン消化，アビジンカラムによるICATタグの精製，タグ切り離し後，ペプチドを脱塩濃縮してナノLC-MS/MSでペプチドの同定・定量を行う．ICATタグ（質量差9）とSILAC標識（質量差6）の組合わせにより，4つの異なる質量をもつペプチドが検出されるので，曝露細胞・対照細胞内の可逆的酸化型・還元型システインを相対定量することができる

れ標識することで区別できるようにした．

具体的には図4に示すように，まずSILAC法を用いて，培養細胞内のリジン，アルギニンを^{13}C体で標識した「重い」細胞と^{12}C体で標識した「軽い」細胞を用意する．どちらかの細胞に酸化剤を曝露後，両細胞を等量混合し，細胞分画を行う．その後，^{13}C体ICATタグで分画中のタンパク質の還元型システイン（-SH）を標識する．次に還元剤（DTTやアスコルビン酸など）で酸化型システインを還元し，^{12}C体ICATタグで標識する．その後，トリプシン消化，アビジンカラムによるICATタグの精製を行い，タグの付いたペプチドを脱塩濃縮してナノLC-MS/MSでペプチドの同定・定量を行う．ICATタグは，9個のCが^{13}Cまたは^{12}Cに置換されているため，^{13}C体ICATタグと^{12}C体ICATタグの質量差は9である．また，トリプシン消化されたSILACペプチドは，6個のCが^{13}Cまたは^{12}Cに置換されたリジンもしくはアルギニンをC末端に有するので，質量差は6である．ICATとSILACによる二重標識の組合わせにより，4つの異なる質量をもつペプチドがMS上で検出されるので，曝露細胞・対照細胞内の酸化型・還元型システインを相対定量することが可能となった．

本法を用いて過酸化水素の標的となるタンパク質のチオール基の探索を行うために，HepG2細胞をSILAC法で標識し，過酸化水素3 mMを15分，45分，90分曝露し，システインの酸化状態を測定した．その結果，シャペロンタンパク質，薬物代謝酵素など，さまざまなタンパク質のチオール基の酸化還元状態が変化していたが，そのなかでもペルオキシレドキシン6（Prx6）の47番目のシステインが顕著に変化した（図5A左）．一方同じ酵素の91番目のシステインは緩やかな反応性を示した（図5A右）．

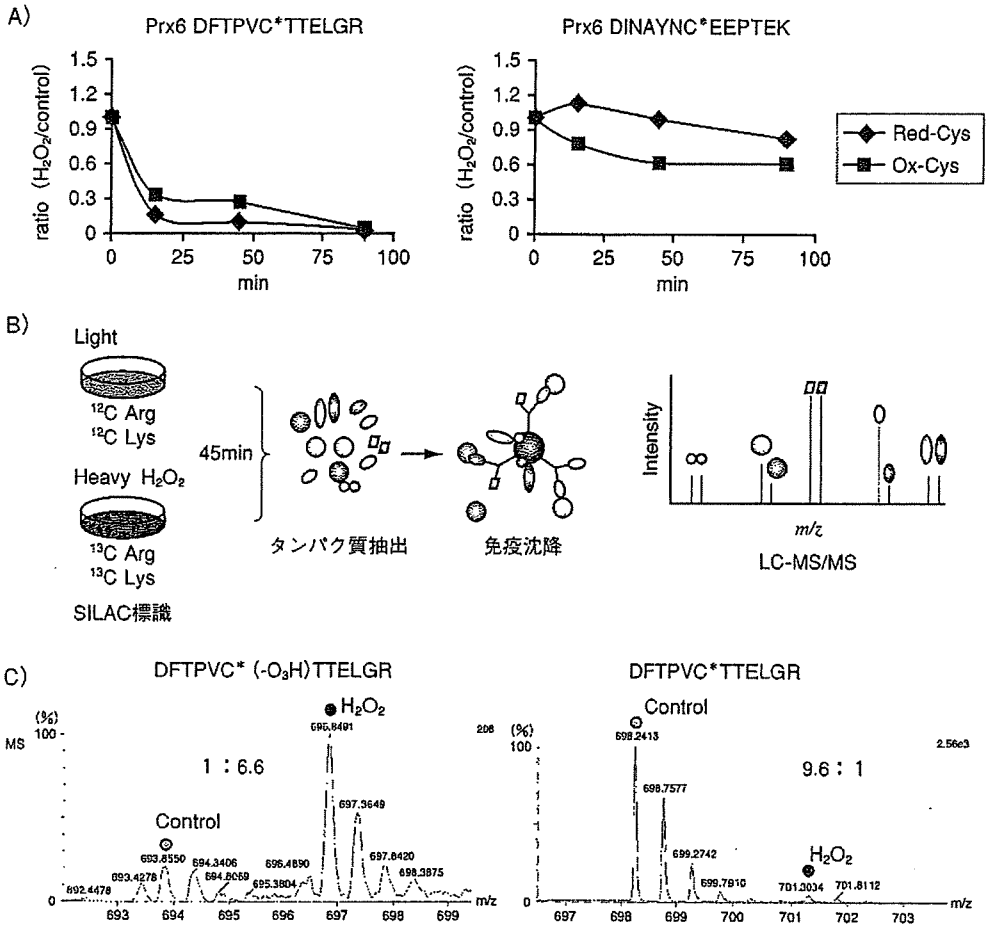

図5　SILAC-IP法によるシステイン修飾構造と修飾部位の特定
A）HepG2細胞を過酸化水素で曝露したときのペルオキシレドキシン6（Prx6）中の可逆的酸化型システイン（Ox-Cys）と還元型システイン（Red-Cys）の経時変化．各グラフ上部に検出対象として同定したシステイン（C*）を含むペプチドのアミノ酸配列を示した．B）C）Prx6抗体を用いたSILAC-IP法．スルフォン化システインが過酸化水素曝露45分後に6.6倍に増加している一方で，還元型＋可逆的酸化型システインが0.1倍に減少している

還元型システイン（Red-Cys）・可逆的酸化型システイン（Ox-Cys）ともに減少していたため，不可逆的酸化型のシステインが増加していることが予想された．そこでPrx6に対象を絞って，免疫沈降法とSILAC法を組合わせた，SILAC-IP法（図5 B）を用いて，不可逆型のシステインの同定・定量を行ったところ，スルフォン化システインが過酸化水素曝露45分後に6.6倍増加している一方で，還元型＋可逆的酸化型システインが0.1倍に減少していることが確認された（図5 C）．このようにDLIAA法とSILAC-IP法との組合わせは，細胞内タンパク質の酸化修飾部位・酸化修飾の種類の同定，また酸化修飾の動態変化を捉えるための有用な手法になるのではないかと考えている．

おわりに

以上，われわれの研究室で開発したDNA付加体およびタンパク質付加体に対するオミクス的アプローチについて紹介した．DNA付加体については，アダクトームマップに現れる未同定のピークの構造決定，およびそのDNA付加体の変異誘発性，修復されやすさ，などのデータを蓄積するのが今後の課題である．一方，DLIAA法は新規のレドックス制御タンパク質の同定研究に役立てたいと考えている．

本稿では触れなかったが，システインの酸化修飾以外にも，膨大な数のタンパク質付加体が存在する．また，RNA付加体に関する研究もいくつか報告されて

いる．これらを網羅的に解析する手法を開発することも今後の課題である．

文献

1）Kim, S. et al.：Chem. Res. Toxicol., 19：852-858, 2006
2）Nair, U. et al.：Free Radic. Biol. Med., 43：1109-1120, 2007
3）Williams, M. V. et al.：J. Biol. Chem., 281：10127-10133, 2006
4）Kasai, H. et al.：Ind. Health, 43：699-701, 2005
5）Kanaly, R. A. et al.：Antioxid. Redox Signal., 8：993-1001, 2006
6）Kanaly, R. A. et al.：Mutat. Res., 625：83-93, 2007
7）Le Moan, N. et al.：J. Biol. Chem., 281：10420-10430, 2006

<筆頭著者プロフィール>

松田知成：京都大学工学研究科博士課程修了．環境汚染物質の毒性メカニズムに広く興味をもっている．2台の質量分析器を駆使して研究に励んでいます．